MOEM

Modern Electronic Materials 2019; 5(3): 107–114
DOI 10.3897/j.moem.5.3.51936

Research Article

Holographic measurement of surface acoustic wave parameters in crystals

Michael E. Gusev[1], Yuri N. Zakharov[2]

1 «Algoritm-Opto Ltd.», 38 Litovsky Val St., Kaliningrad, 236016, Russia
2 Harvard University, 330 Brookline Ave., Boston, MA 02215, USA

Corresponding author: Yuri N. Zakharov (yz-ua3@list.ru)

Received 13 August 2019 ♦ **Accepted** 5 September 2019 ♦ **Published** 12 September 2019

Citation: Gusev ME, Zakharov YuN (2019) Holographic measurement of surface acoustic wave parameters in crystals. Modern Electronic Materials 5(3): 107–114. https://doi.org/10.3897/j.moem.5.3.51936

Abstract

The theoretical basis of a specialized technique for applying digital holographic interferometry to measure the parameters of surface acoustic waves is presented, a measuring system for visualization and quantitative analysis of the parameters of ultralow-amplitude high-frequency oscillations arising in electronic devices using surface acoustic waves is developed, and experimental results of the study of surface acoustic waves in crystals of lithium niobate are obtained. In this case, to ensure the possibility of recording precision double-exposure interferograms of high-frequency surface acoustic waves, a picosecond pulsed laser with two-stage frequency multiplication was used as a radiation source, and to increase the spatial resolution of the system with the possibility of observing a wide field of view, an adjustable optical zoom of the incoming image was applied to the matrix input (based on charge-coupled devices) of the recording camera and digital zoom was used for obtained interferogram. We achieved the measuring sensitivity of the surface acoustic waves amplitude and spatial-temporal resolution allowing visualization and measurement of surface acoustic waves with amplitudes of the order of 1 nm and frequencies of the order of 10 MHz, which is far beyond the capabilities of standard methods of holographic interferometry.

Keywords

surface acoustic waves, holographic interferometry, digital holography

1. Introduction

Finding the optimum conditions for the formation, propagation and reflection of surface acoustic waves **(SAW)** provides the possibility of greatly improving the performance of advanced electronic devices employing this physical phenomenon. Typical methods are based on measurements of secondary wave parameters with point detectors at discrete locations and are followed by calculations of wave amplitude, frequency and phase parameters [1–5].

It is well-known however that the holographic interferometry method has unique advantages from the viewpoint of visualization and measurement of surface microdeformation [5]. Laser frequency multiplication additionally increases the sensitivity of measurements [6]. In fact it allows simultaneous SAW visualization across the entire surface [7] studied and direct measurement of wave parameters (wavelength, amplitude and oscillation pattern) [8, 9]. However existing holographic measuring systems do not deliver the required time and spatial resolution for the visualization and parameter measurement

of high-frequency ultralow amplitude oscillations generated by SAW [10].

In this work we analyze results of theoretical and experimental studies aimed at the development of special holographic equipment and method for SAW parameter measurement in solids.

2. Theoretical basis of holographic measurement method

2.1 Limit longitudinal spatial resolution of method (interferometer motion sensitivity)

One of the most important factors limiting the applications of holographic interferometry for measurements of nanometer-scale surface motions is the sensitivity of a holographic interferometer an assessment of which will be given below.

The operation principle of a holographic interferometer is as follows. Laser radiation is split into the object beam which illuminates the object and the reference beam directed to the input sensor of the digital video camera. The object beam illuminates the object in the direction $\mathbf{k}_i$. The portion of light reflected by the object in the direction $\mathbf{k}_v$ referred to as the observation direction passes through an optical focusing system and forms an image of the object at the input sensor of the camera. An image domain hologram forms on the CCD matrix of the digital camera as a result of interference between the reference and object beams.

Let $R(x, y)$ be the flat reference wave and $U(x, y)$ the object reflected wave. Then the intensity at the CCD matrix can be described as follows [10]:

$$I_H(x, y) = |R_H(x, y)|^2 + |U_H(x, y)|^2 + R_H(x, y)U^*_H(x, y) + R^*_H(x, y)U_H(x, y), \quad (1)$$

where H is the hologram plane index and * is the complex conjugation index. The intensity described by Eq. (1) is detected by a 2D electronic device incorporating multiple arrays of sensitive cells ($M \times N$ pixels) having the size $\Delta x \times \Delta y$, thus allowing one to describe the intensity in the form of the function $I_H(m \times x, n \times y)$ where m и n are integers. The last two terms of Eq. (1) contain information on the amplitude and phase of the object wave. This information can be separated by means of spatial filtering using Fourier transform [11]. Fourier transform of the detected array allows separating and filtering one of the last two terms in Eq. (1). These terms are separated in the Fourier plane by slight tilting of the reference beam relative to the object one. Filtering and inverse Fourier transformation yield the complex amplitude of the object wavefront. The digital complex amplitude $U_H(m\Delta x, n\Delta y)$ can be used for calculating the phase of the object wavefront:

$$\varphi_H(m\Delta x,\ n\Delta y) = \operatorname{arctg}\frac{\operatorname{Im}\left[U_H(m\Delta x, n\Delta y)\right]}{\operatorname{Re}\left[U_H(m\Delta x, n\Delta y)\right]}, \quad (2)$$

where Re and Im are the real and imaginary parts of the complex number, respectively. Deduction of the phases of the object fields calculated for two states of the object get the phase difference from which once can calculated the shift of the points of the object **u** in the direction **s** resulting from the application of a load:

$$\Delta\varphi = \frac{2\pi}{\lambda}\mathbf{us}, \quad (3)$$

where λ is the laser wavelength, **s** is the interferometer sensitivity vector described as $\mathbf{s} = \mathbf{k_i} - \mathbf{k_v}$ and $\mathbf{k_i}$ and $\mathbf{k_v}$ are the unit vectors of the illumination and observation directions, respectively.

It follows from Eq. (3) that the maximum system sensitivity to motions in the surface normal direction (which are the case for SAW) is achieved if the illumination and observation directions are normal to the surface ($|\mathbf{s}| = 2$). Each fringe in the interference pattern has the value λ/2, where λ is the laser wavelength, and this value determines the sensitivity of the interferometer (in the optical region this is 350–200 nm per fringe). If the surface motion range is within λ/2 no fringes form in the interference pattern but the phase distribution in the object waves of two holograms and their phase difference can be calculated from the information derived from discrete pixels of the CCD matrix. The limit sensitivity in this case is determined by the minimum surface shift in the direction of the interferometer sensitivity vector which causes a response of the measuring system.

As follows from Eq. (3) the sensitivity of the holography method is inversely proportional to the laser wavelength used for hologram writing which is well-known for high accuracy (to within the spectral width which is of the order of tens of femtoseconds for holographic lasers). However knowing this fact alone does not allow judging about the minimum dimension of the detected motions.

The basic factor determining the limit sensitivity of a specific design of a holographic measuring system is the resolution of the measuring system which contains multiple components, including the recording CCD matrix, the circuitry and the software. If holograms are recorded and processed with 8-bit digital devices and software the measuring system will finally provide for a 256-grade division of the maximum surface shift magnitude W_{max} calculated from the interference pattern, so the value of each grade is as follows:

$$\Delta W = \frac{W_{max}}{256}. \quad (4)$$

Then the measurement data (motion field) are represented as a discrete function of two variables $W = F(m\Delta x, n\Delta y)$, where Δx and Δy are the pixel dimensions in the image and m and n describe the sequence number of a pixel in each of the axes. The value of the function W is constant within each pixel and is a multiple of ΔW. It follows from Eq. (4) that with a decrease in the overall magnitude of object shift the value of the grade ΔW decreases and

becomes the smallest if the interference pattern contains one fringe. As shown above if the optical setup of the interferometer has normal illumination and observation directions the value of one interference fringe is λ/2. Thence the value of one grade or the minimum surface shift magnitude that can be detected by the system (a change to the next grade) can be calculated for this case as follows:

$$\Delta W_{\min} = \frac{0,5\lambda}{256}. \quad (5)$$

Due to the specific features of the data digitalization systems used in most experimental instruments the value of one grade calculated with Eq. (5) remains the same regardless of further decrease in the overall shift in the interference pattern (to within portions of a fringe). Thus motions that are smaller in magnitude than the values calculated above will not cause any response of the measuring system. Therefore these values can be accepted as the limit resolution of the measuring system for a specific laser wavelength. It follows from Eq. (5) that the theoretical limit sensitivity of the method for hologram recording with ultraviolet radiation is less than 1 nm. However Eq. (1) does not allow for speckle noise generated by coherent light reflection from surfaces of diffuse reflecting objects. In practice the abovementioned limit sensitivity is only achievable for measurement of motions of objects with mirror surfaces that do not produce high-frequency speckle-structure in the reflected object wave.

2.2 Time resolution of method

Another most important factor limiting the use of holographic interferometry for studies of dynamic processes is the frequency of test object surface oscillations. There are publictions on the application of holographic interferometry for measurement of oscillations at up to 100 kHz frequencies [12]. Data on holographic visualization or measurement of higher frequency oscillations are unavailable.

Double-exposure interferometry of an oscillating object incorporates recording and interferometric comparison between two holograms one of which is taken for the specimen in rest and the other is recorded after oscillations were generated in the specimen. A most important factor determining the fringe contrast and the measurability of the oscillations is the on-off time ratio k described as follows:

$$k = \frac{T}{t}, \quad (6)$$

where T is the object surface oscillation period and t is the exposure time (hologram recording time).

It is well-known that in order for a double-exposure interference pattern of an oscillating surface to become recordable at an oscillation amplitude that is equal to or smaller than the laser wavelength, the on-off time ratio should be at least 10. For standing waves exposure should be synchronized with the onset of surface oscillation phase [13].

The exposure time of CCD matrices in conventional holographic interferometers with cw laser irradiation [14] is software-set to within 1/15–1/20000 s, i.e., $k = 10$ can be provided for oscillation frequencies of within 2 kHz. Using these systems for measurements of object surface oscillations at frequencies typical of SAW (up to 1 GHz) will make the on-off time ratio far smaller than one.

At $k << 1$ the object wave intensity is averaged over oscillating object exposure time [15, 16, 17]. Comparing this hologram with one taken in rest produces the so-called quasi-binary interference pattern [18] which does not allow visualization and parameter measurement of oscillations with amplitudes of less than λ/2 since the interference pattern will not show the respective intensity gradient.

Thus theoretical analysis results in a conventional holographic interferometer does not allow visualization and parameter measurement of oscillations at MHz frequencies due to its long exposure time. To provide for the required on-off time ratio at oscillation frequencies of up to 1 GHz (oscillation period 1 ns) the exposure time should be within 100 ps.

2.3 Transverse spatial resolution

Accepting that SAW-caused motions (deformations) of object surface generate small phase fluctuations of the reflected light wave in one direction one can assume that the interference pattern of specimen surface oscillations will be in the form of a system of parallel low-contrast fringes perpendicular to the SAW propagation direction. If the hologram is recorded with an 1× magnification optical system the phase gradient period in the interference pattern (fringe step) will be equal to the SAW wavelength.

Since holograms are written with CCD matrices the unit resolution will be determined by the CCD matrix pixel size which is at least 5 μm for conventional high resolution cameras.

Basically, to allow recording an interference pattern onto a CCD matrix the division step (pixel size) should be at least 2 times smaller than the fringe step in the interference pattern [10].

One can easily calculate that for a 4000 mps sound velocity in a lithium niobate crystal this criterion is met for SAW frequencies of up to 400 MHz at which there are 2 pixels per wavelength. At higher frequencies the Nyquist criterion is not met. Furthermore the too small number of pixels per wavelength for SAW frequencies of 10–400 MHz is obviously insufficient for plotting a smooth envelope curve of oscillation motions which is a decisive factor in measurements of wave parameters (wavelength and amplitude). Therefore measuring the parameters of high-frequency SAW requires image magnification at CCD matrix input.

It is also noteworthy that measuring oscillation motion fields for SAW is in fact a self-contradictory task. For example, whereas visualization of a SAW across the entire specimen surface requires the largest observation zone

available be provided (minimum image magnification), achieving the highest accuracy of SAW parameter measurements requires maximum magnification thus narrowing the object surface area taken within one exposure time.

To overcome this contradiction and provide for the maximum adaptability of the measuring system one can use a combined two-step image magnification system.

1. Optical image magnification upon hologram recording at CCD matrix input with the magnification factor being adjustable in a range of 2×–10×. This will, on the one hand, provide SAW visualization over the maximum available surface area and, on the other hand, acquire a sufficient array of data for further SAW parameter measurements.
2. Computer image scaling with an up to 20× factor allowing the operator to select, magnify and process an interference pattern of interest after SAW visualization to achieve maximum accuracy of SAW parameters (wavelength and amplitude) in any specimen surface area as may be required.

3. Experimental

The test specimen was a 50 × 50 × 3 mm^3 one-side polished lithium niobate wafer. SAW were excited in the specimen and the response was measured with the interdigital transducers **(IDT)** D1–D8 applied onto the specimen surface by lithography. The specimen is schematically shown in Fig. 1.

The radiation source of the experimental setup (Fig. 2) was a passively mode-locked picosecond-pulse yttrium-aluminum garnet laser. The master generator 2 of the laser was a 50 ps single pulse output circuit. The first harmonic wavelength was 1.063 μm, the beam cross-section being ~1.5 mm. The master generator signal was amplified by a two-pass optical amplifier 3. The amplifier output pulse energy was 2–3 mJ. The output beam cross-section was ~2 mm, the coherent length being ~3–5 m. After the output of the amplifier 3 the radiation was directed to a 2 mm thick nonlinear potassium titanyl phosphate crystal 4 in which the 1.063 μm radiation was converted with a 30% efficiency to the second harmonic (0.532 μm). Then the 0.354 μm third harmonic was generated by a potassium dihydrophosphate crystal 5 and a UV filter 6 which cut off the 1.063 and 0.532 μm harmonics. Then the 0.354 μm radiation was converted by a collimator 13 to an adjustable cross-section parallel beam and directed to a holographic interferometer 7 and further to the test specimen 9 and a CCD camera 8. The CCD camera was synchronized with laser pulses by a signal which was output from the laser excitation unit 1 at the onset of excitation lamp ignition and switched the camera to standby mode. After exposure each frame was stored in memory for a preset time. The CCD camera was controlled by a computer 10 with special software for hologram recording and calculation and processing of digital holographic interference

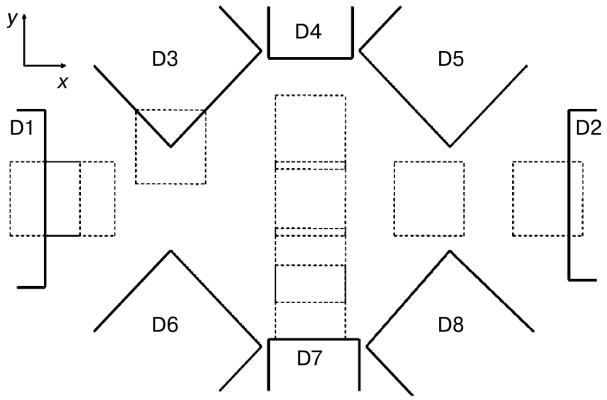

Figure 1. Schematic of test object showing positions of IDTs D1–D8. Dashes show measurement areas.

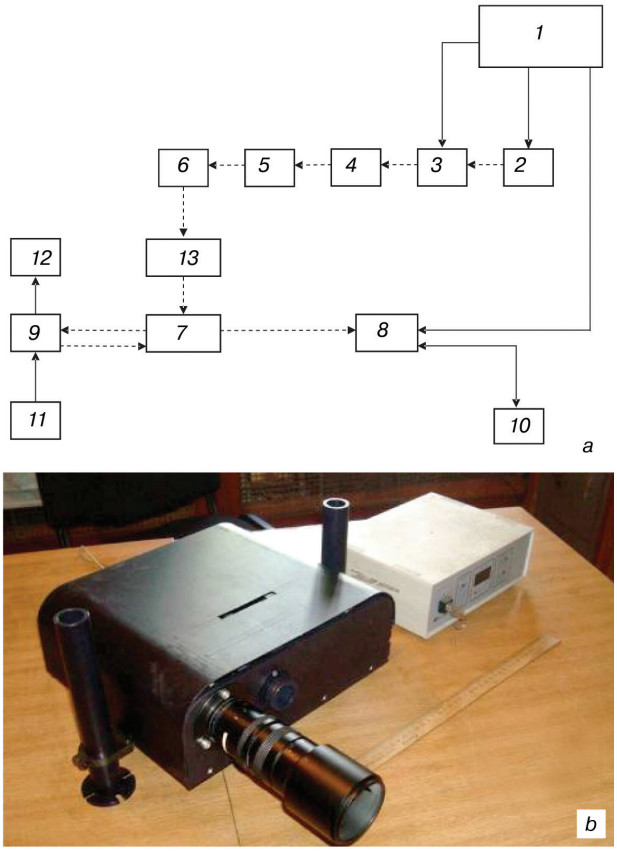

Figure 2. (*a*) Schematic diagram of experimental setup and (*b*) general appearance of digital holographic interferometer.

patterns. A generator 11 excited SAW in the specimen and an oscilloscope 12 controlled the presence of SAW and selected resonance frequencies. Solid arrows in Fig. 2 show electric conections and dashed arrows show optical path.

The measurement sequence was as follows.

3.1 Measurement system assembly and setup

The parameters of the optical system were selected experimentally with the criterion of optimum hologram recording conditions. SAW were excited by sending an electric signal from the high-frequency generator to the IDT D1.

Resonance was tuned by the maximum signal magnitude read by the oscilloscope connected to the IDT D2. The resonance frequency measured was f_0 = 17 MHz. Two conventional measuring devices were used (a Tektronix TDS 303 2B oscilloscope and G3-19A and G-102A generators).

3.2. Specimen hologram recording

In rest (without load) holograms were recorded using a 50 ps pulse laser at λ_3 = 0.354 μm. The subsequent series of holograms in excited state at the resonance frequency were recorded with 5–30 s intervals between exposures. Loaded specimen holograms for each measurement area (Fig. 1) were recorded in excited state at the resonance frequency at 10–15 V in two modes:

- IDTs D2–D8 shorted (SC mode);
- IDTs D2–D8 under 50 Ohm matching load.

To record interference patterns in all the measurement areas shown in Fig. 1 we moved the specimen in its plane with a precision XY moving platform after recording each series of holograms at a selected area, and then recorded holograms for the next area.

3.3. Recording and quantification (analysis) of double-exposure digital holographic interference patterns

The interference patterns were recorded with special hologram processing software providing interference comparison of two holograms and subsequent motion field calculation. The holograms being compared were one for an in-rest object and the other for an excited object.

3.4. Superposition of interference patterns with respective specimen surface areas (Fig. 3)

Aimed at analyzing the overall SAW propagation pattern on the specimen surface.

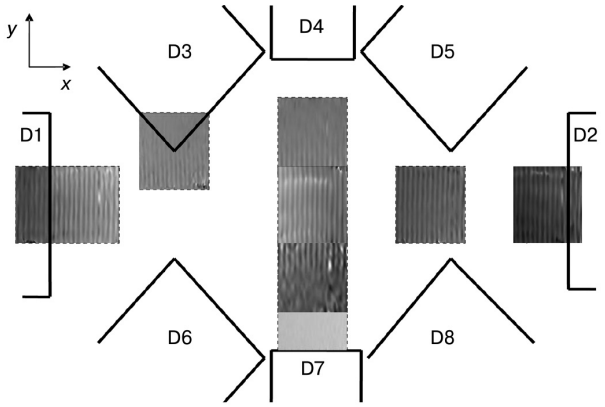

Figure 3. Visualization of SAW on specimen surface.

4. Results and discussion

Figure 3 shows the final SAW visualization result obtained by processing of a series of interference patterns for a 2.7× system magnification (recording area size 3.25 × 3.25 mm^2) and providing information on SAW propagation across the entire specimen surface. Analysis results the following:

- the SAW propagate within a limited area, i.e., a strip shaped fragment of the specimen surface spreading between the IDT D1 and the IDT D2 in length and between the extreme points of the IDTs D3–D6 in width;
- the SAW wavefront is flat and remains parallel to the output edge of the exciting IDT D1 throughout the whole propagation distance until the IDT D2 input edge;
- the specimen surface scanning method in which the specimen is moved between measurement areas with an XY moving platform provides the possibility of visualization and parameter measurement of SAW across the entire specimen surface by stitching interference patterns.

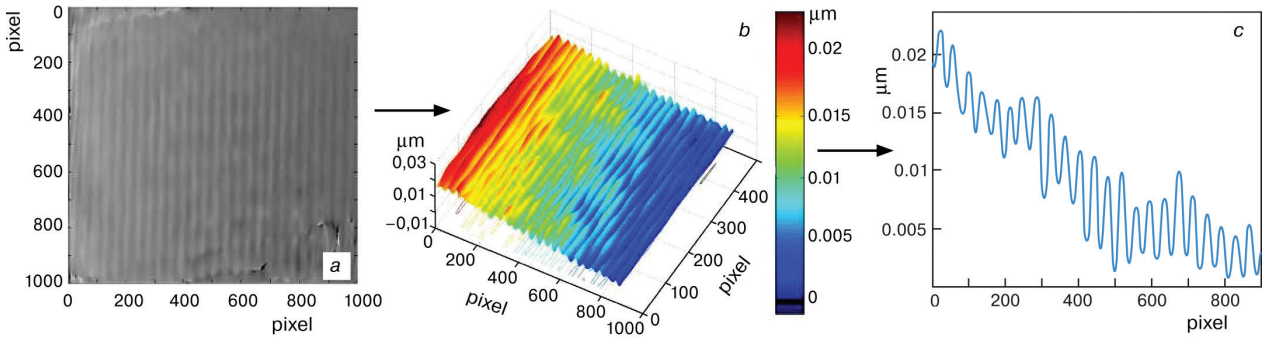

Figure 4. Visualization of SAW in specimen center under thermal deformations: (*a*) interference pattern, (*b*) restored motion field and (*c*) vertical section of motion field in wave vector plane (*a* and *b*: 1.5× magnification (1000 × 1000 pixels along horizontal axes correspond to 6 × 6 mm^2); *b* and *c*: surface shift in vertical plane, μm).

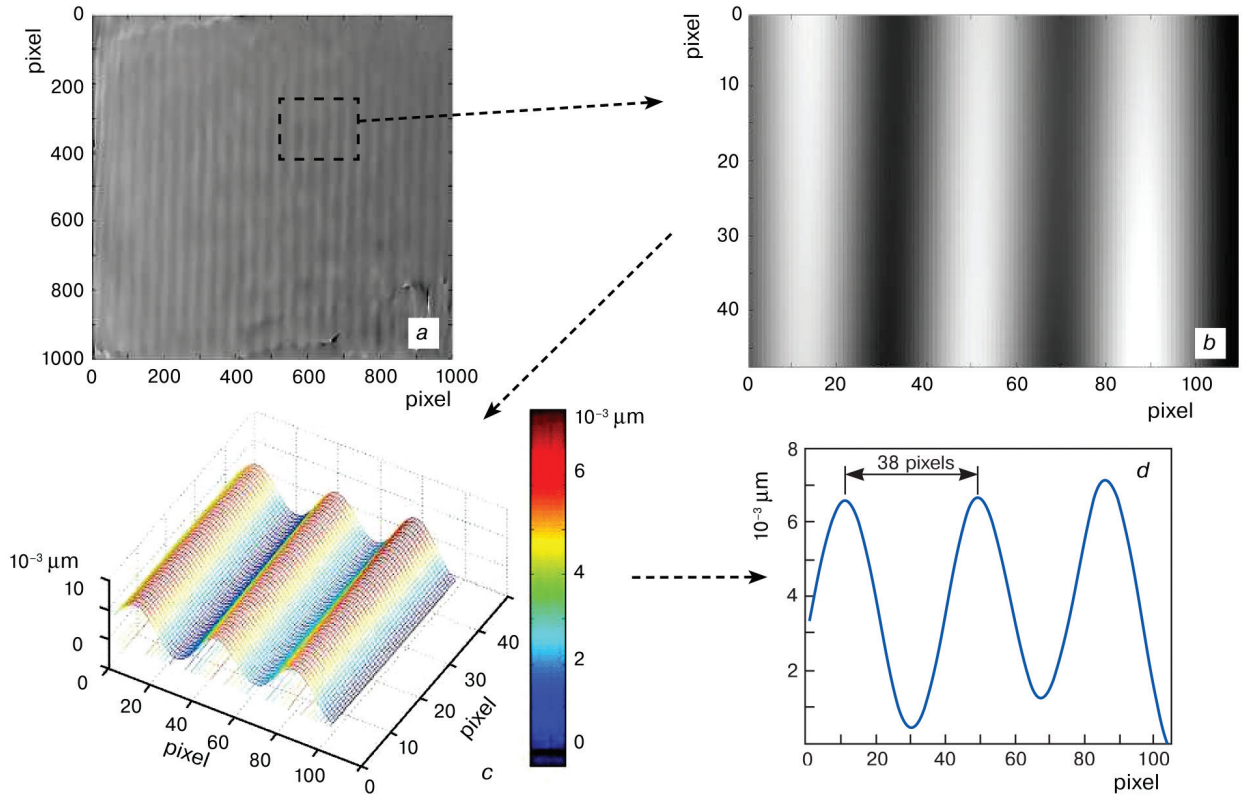

Figure 5. SAW parameters measured in specimen center for excitation by IDT D1 at 17 MHz and in SC mode: (*a*) interference pattern, (*b*) digital magnification of selected area in the interference pattern (*a*); (*c*) restored motion field and (*d*) vertical section of motion field in wave vector direction. Magnification 1.5× (pixel size 6 µm). SAW length: 38 pixels × 6 µm = 240 µm, SAW amplitude: 3–3.5 nm.

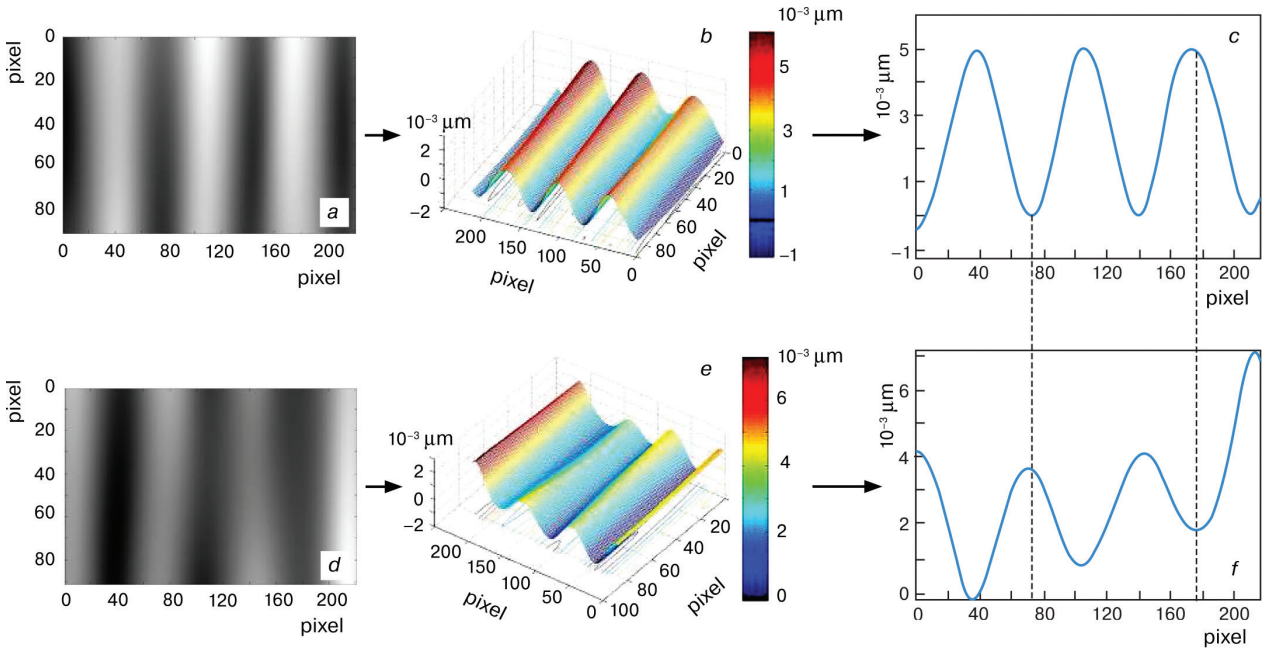

Figure 6. SAW type check in SC mode by comparing surface motion functions for a specimen area at different arbitrary moments of time: (*a* and *d*) interference patterns, (*b* and *e*) restored motion field and (*c* and *f*) vertical section of restored motion field. Recording instant for the top figures differs from that for the bottom figures by an arbitrary value.

To check the possibility of enlarging the observation area per one recording cycle and hence decreasing the number of recording cycles required for visualization of the entire specimen surface we experimented with recording 1.5 : 1 scale holograms in the specimen center. The area recorded per time was 6 × 6 mm^2. The resultant interference patterns showed that the spatial resolution of the CCD matrix provides for clear visualization of SAW with this magnification at the test oscillation frequency. To check hologram recording quality we also quantified the interference patterns and as a result found that the entire surface was tilted due to specimen thermal expansion (Fig. 4), and measured basic SAW parameters. The measured data agree well with the calculations (Fig. 5).

To determine whether the SAW were standing or traveling we compared the motion functions of one specimen surface area calculated from interference patterns recorded at different arbitrary moments of time. For standing waves the locations of the oscillation loops (peaks of motion function) on the specimen surface should not change in time. Comparison for excitation in SC mode results the waves were standing (Fig. 6). It can be seen from the curves shown in Fig. 6 that at the recording instants the surface shifts caused by the SAW were in phase opposition but the locations of the oscillation loops remained the same suggesting the wave was standing.

5. Conclusion

Visualization and parameter measurement of high-frequency acoustic waves in a lithium niobate crystal by means of digital holographic interferometry showed that subject to special measures this method provides the following results:

- shift sensitivity of within 1 nm;
- time resolution providing for measurement of fast deformations at frequencies of at least tens of MHz (with a potential for up to 5 GHz);
- spatial resolution providing for measurements in microscopic areas, i.e., tens of microns (50 × 50 μm^2 in our experiments).

These limiting parameters of digital holographic interferometry are far better than the applicability limits of conventional holographic interferometry.

The reported experimental limit sensitivity and resolution of the digital holographic interferometry method can be significantly improved through special measures. For example, to improve the sensitivity limit one can use UV lasers for recording digital holograms alongside with cameras and software providing a greater number of grades in image digitizing. To improve the time resolution of the method one can use femtosecond laser pulses. The spatial resolution of the method can be further improved by recording holograms onto CCD matrices with a greater number and smaller sizes of pixels (for example FL3-U3-120S3C-C (FLIR Systems, Inc.) [19]).

Our results confirm that digital holographic interferometry is a promising tool for coherent optical measurements of high-frequency SAW parameters. These results lay the foundation for developing an industrial technology and a variety of measuring devices offering unique measurement capabilities in the solution of a broad range of problems related to SAW electronic components.

References

1. Komotskii V.A., Okoth S.M. Measuring reflections of surface acoustic waves from periodical set of stripes using laser beam probing method. *Vestnik RUDN. Seriya Fizika*. 2002; 10(1): 144–147. (In Russ.)
2. Komotskii V.A., Sokolov Yu.M., Basistyi E.V. Method for measuring the depth of periodic relief reflectors of surface acoustic waves by laser sounding. *Radiotekhnika i elektronika*. 2011; 56(2): 243–248. (In Russ.) https://doi.org/10.1134/S1064226910121125
3. Komotskii V.A., Kuznetsov M.V., Okoth S.M. Measuring thickness of thin metallic films with the use of laser probing technique. *Vestnik RUDN. Seriya Fizika*. 2005; (1): 48–53.
4. Dolbischenko V.V., Derkachenko E.V., Danilov V.V. The generalized structure of hardware for measuring the parameters of surface acoustic waves. In: Materials of the international scientific-practical conference «Modern information and electronic technologies». Odessa, 2005: 274. (In Russ.)
5. Biryukov D.Yu., Vladimirov A.P., Eremin P.S., Zatsepin A.F., Kortov V.S., Mitrokhin A.A. The use of laser interferometry for non-contact measurement of the velocity of Rayleigh waves in optical glass. In: XVII Russian Scientific and Technical Conference «Non-Destructive Testing and Diagnostics». Ekaterinburg: Ural, 2005. (In Russ.)
6. Redkorechev V.I., Kulagin I.A., Gurevich V.S., Gusev M.E., Zakharov Yu.N. Picosecond three-color holographic digital interferometry. *Opt. Spectrosc*., 2009; 107(3): 407–411. https://doi.org/10.1134/S0030400X09090161
7. Rambach R.W., Taiber J., Scheck C.M.L., Meyer C., Reboud J., Cooper J.M., Frankea T. Visualization of surface acoustic waves in thin liquid films. *Sci. Rep.*, 2016; 6: 21980–1–8. https://doi.org/10.1038/srep21980
8. Bruno F., Laurent J., Royer D., Atlan M. Holographic imaging of surface acoustic waves. *Appl. Phys. Lett.*, 2014; 104(8): 083504. https://doi.org/10.1063/1.4866390
9. Leclercq M., Picart P., Penelet G., Tournat V. Investigation of 3D surface acoustic waves in granular media with 3-color digital holography. *J. Appl. Phys.*, 2017; 121(4): 045112 1–10. https://doi.org/10.1063/1.4974950
10. Schnars U., Jüptner W. Digital Holography. In: Digital Hologram Recording, Numerical Reconstruction, and Related Techniques.

Berlin; Heidelberg: Springer-Verlag, 2005, 164 p. https://doi.org/10.1007/b138284

11. Alexeenko I., Gusev M., Gurevich V. Separate recording of rationally related vibration frequencies using digital stroboscopic holographic interferometry. *Appl. Opt.*, 2009; 48(18): 3475–3480. https://doi.org/10.1364/AO.48.003475
12. Deason V.A., Telchow K.L., Watson S. Imaging of acoustic waves in sand. Idaho Falls (US), 2003. https://doi.org/10.1117/12.504832
13. Ostrovsky Yu.I., Butusov M.M., Ostrovskaya G.V. *Golograficheskaya interferometriya* [Holographic interferometry]. Moscow: Nauka, 1977, 336 p. (In Russ.)
14. Pedrini G., Osten W., Gusev M. High-speed digital holographic interferometry for vibration measurement. *Appl. Opt.*, 2006; 45(15): 3456–3462. https://doi.org/10.1364/AO.45.003456
15. Powell R.L., Stetson K.A. Interferometric vibration analysis by wavefront reconstruction. *JOSA*, 1965; 55(12): 1593–1598. https://doi.org/10.1364/JOSA.55.001593
16. Collier R.J., Burckhardt C.D., Lin L.H. Optical Holography. New York: Academic Press, 1971, 621 p. https://doi.org/10.1016/B978-0-12-181050-4.X5001-X
17. Zakharov Yu.N. Surface acoustic waves investigation with the help of time-average digital holography. *Opt. Mem. Neural Networks*, 2008; 17(4): 286–288. https://doi.org/10.3103/S1060992X08040073
18. Borza D. Vibration amplitude field estimation based on high-resolution time-averaged Interferograms. *Proc. of SPIE*, 2006; 6341(06): 6341241-6. https://doi.org/10.1117/12.695379
19. FLIR Systems. https://www.flir.com/products/flea3-usb3